Cationic PAMAM Dendrimers Aggressively Initiate Blood Clot Formation

Clinton F. Jones,[†,▽] Robert A. Campbell,[‡,▽] Amanda E. Brooks,[†] Shoeleh Assemi,[§] Soheyl Tadjiki,[⊥] Giridhar Thiagarajan,[#,△] Cheyanne Mulcock,[†] Andrew S. Weyrich,[‡,∥] Benjamin D. Brooks,[†] Hamidreza Ghandehari,[†,#,△] and David W. Grainger[†,#,△,*]

[†]Department of Pharmaceutics and Pharmaceutical Chemistry, Health Sciences, University of Utah, Salt Lake City, Utah 84112, United States, [‡]Program in Molecular Medicine, University of Utah School of Medicine, Salt Lake City, Utah 84132, United States, [§]Department of Metallurgical Engineering, University of Utah, Salt Lake City, Utah 84112, United States, [⊥]Postnova Analytics, Inc., Salt Lake City, Utah 84102, United States, [∥]Divisions of Pulmonary and Critical Care Medicine, Department of Internal Medicine, University of Utah, Salt Lake City, Utah 84132, United States, [#]Utah Center for Nanomedicine, Nano Institute of Utah, University of Utah, Salt Lake City, Utah 84112, United States, and [△]Department of Bioengineering, University of Utah, Salt Lake City, Utah 84112, United States. [▽]These authors contributed equally to this work.

ABSTRACT Poly(amidoamine) (PAMAM) dendrimers are increasingly studied as model nanoparticles for a variety of biomedical applications, notably in systemic administrations. However, with respect to blood-contacting applications, amine-terminated dendrimers have recently been shown to activate platelets and cause a fatal, disseminated intravascular coagulation (DIC)-like condition in mice and rats. We here demonstrate that, upon addition to blood, cationic G7 PAMAM dendrimers induce fibrinogen aggregation, which may contribute to the *in vivo* DIC-like phenomenon. We demonstrate that amine-terminated dendrimers act directly on fibrinogen in a thrombin-independent manner to generate dense, high-molecular-weight fibrinogen aggregates with minimal fibrin fibril formation. In addition, we hypothesize this clot-like behavior is likely mediated by electrostatic interactions between the densely charged cationic dendrimer surface and negatively charged fibrinogen domains. Interestingly, cationic dendrimers also induced aggregation of albumin, suggesting that many negatively charged blood proteins may be affected by cationic dendrimers. To investigate this further, zebrafish embryos were employed to more specifically determine the speed of this phenomenon and the pathway- and dose-dependency of the resulting vascular occlusion phenotype. These novel findings show that G7 PAMAM dendrimers significantly and adversely impact many blood components to produce rapid coagulation and strongly suggest that these effects are independent of classic coagulation mechanisms. These results also strongly suggest the need to fully characterize amine-terminated PAMAM dendrimers in regard to their adverse effects on both coagulation and platelets, which may contribute to blood toxicity.

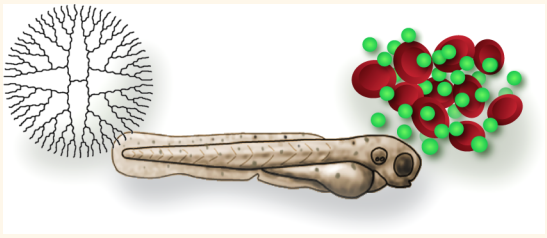

KEYWORDS: nanotoxicity · fibrinogen · protein aggregation · blood compatibility · coagulation · surface charge

Nanoparticles and other nanotechnologies promise to address a broad cross-section of biomedical needs in diverse applications such as drug delivery systems, imaging agents, and diagnostic products.[1] Medical nanotechnology markets are predicted to exceed $53 billion globally in 2012, and nanotechnology is projected to provide a component in up to half of all pharmaceutical products by 2015.[2] Dendrimers, a class of progressively hyperbranched polymers with diverse chemistries and unique properties, are proposed to be an important component in future innovations and applications of nanomaterials in medicine.[3] Their dendritic polymer structure provides highly versatile chemistry with monodisperse, multifunctional properties from geometrically and size-controlled molecules bearing high densities of terminal functional groups. Drug delivery applications for dendrimers are receiving increasing focus especially in two research areas: (1) as drug conjugates, in particular in cancer therapeutics,[4,5] and (2) as a drug solubilization technique.[6,7] Notably, both of these applications could yield new drug formulations containing dendrimers with many possible routes of *in vivo* administration, significant bioavailability, and systemic exposure in humans.

Recently, amine-terminated (PAMAM) dendrimers were shown to exhibit potent

* Address correspondence to david.grainger@utah.edu.

Received for review August 1, 2012 and accepted October 12, 2012.

Published online October 13, 2012
10.1021/nn303472r

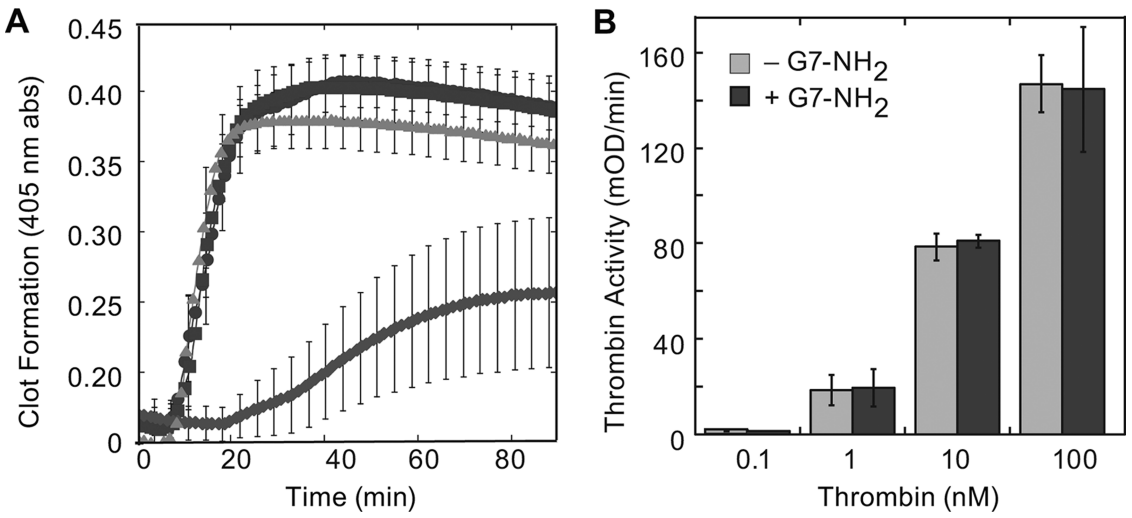

Figure 1. Cationic dendrimers blunt fibrin clot formation, but have little effect on thrombin activity. PPP was harvested as described in Methods, and clot formation induced by the addition of recombinant tissue factor (Innovin 1:10000, final) and calcium (20 mM) (triangle). In some reactions, G6.5-COOH (square), G7-OH (circle), or G7-NH_2 (diamond) (100 μg/mL, final) was added immediately before initiation of the reaction (A). To test whether cationic dendrimers directly affected the ability of thrombin to cleave fibrinogen, G7-NH_2 dendrimers were incubated with various concentrations of thrombin. The ability of thrombin to cleave a chromogenic substrate was then measured by a spectrometric plate reader at 405 nm (B).

activation reactions in whole blood, producing nanotoxicity.[8−13] Specifically, cationic dendrimers have recently been shown to extensively activate platelets, induce platelet aggregation, and comprehensively modify platelet functions both *in vitro* and *in vivo*.[8,13] Notably, some observed mechanisms of dendrimer pro-coagulant functions are unusual: cationic generation-7 PAMAM dendrimer (G7-NH_2) inhibited platelet-supported thrombin generation. Previous findings have further documented the dependence of these observed dendrimer−platelet effects on dendrimer formal surface charge and charge density that promote direct dendrimer binding to platelets and extensive platelet morphological alterations.[8,13] In rodents, intravenously injected cationic dendrimers were observed to produce a disseminated intravascular coagulation (DIC)-like condition accompanied by production of fibrinogen degradation products and rapid mortality.[14] The contrast of this fatal coagulopathy *in vivo* with observations of dendrimer inhibition of thrombin generation *in vitro* is unique and intriguing, but currently without any mechanistic understanding. This potent cationic dendrimer toxicity in blood requires further elucidation of dendrimer interactions with the coagulation cascade and its end product, the fibrin clot.

In this study, we demonstrate interactions of charge-dense, cationic (−NH_2-terminated) high-generation dendrimers with fibrinogen to generate clot-like structures. Results provide novel mechanistic data to demonstrate that cationic dendrimers induce coagulopathies through their ability to aggregate negatively charged blood proteins, including fibrinogen and albumin. Furthermore, real-time intravital observations in zebrafish embryos (ZFEs) expand previous *in vivo* observations with temporal refinement of the clot-like effect and demonstrate the significance of the formation of dendrimer-induced fibrinogen aggregation that is independent of classic coagulation pathways. Taken together, these results strongly suggest a mechanism of rapid, extensive electrostatic interaction to produce the DIC-like phenomena when densely charged cationic dendrimers contact blood.

RESULTS

Previous observations of rapid, dose-dependent *in vivo* coagulation[14] prompted by high-generation cationic dendrimer intravenous injection have no known mechanism. Attempts to better understand the interactions of these cationic dendrimers with blood components began by examining dendrimer effects on clot formation. Recombinant tissue factor and calcium chloride were added to platelet-poor plasma (PPP) in the absence or presence of G7-NH_2, G7-OH, or G6.5-COOH dendrimers. Clot formation was monitored by changes in turbidity measured at 405 nm. Figure 1A shows that cationic dendrimer-treated plasma clots formed substantially slower and to a lesser extent than both saline-treated negative controls and anionic/neutral dendrimer-treated samples. These results agree with the previous finding that cationic dendrimers inhibit thrombin generation *in vitro* in whole blood and platelet-rich plasma,[13] but seem to contradict the previous *in vivo* observations of coagulopathy.[14]

Our previous results suggested that thrombin generation was blunted in plasma in the presence of cationic dendrimer, but did not preclude the possibility for blunted thrombin activity in the presence of G7-NH_2. To determine if thrombin activity is affected, incresasing concentrations of thrombin were preincubated with a constant concentration of cationic dendrimer,

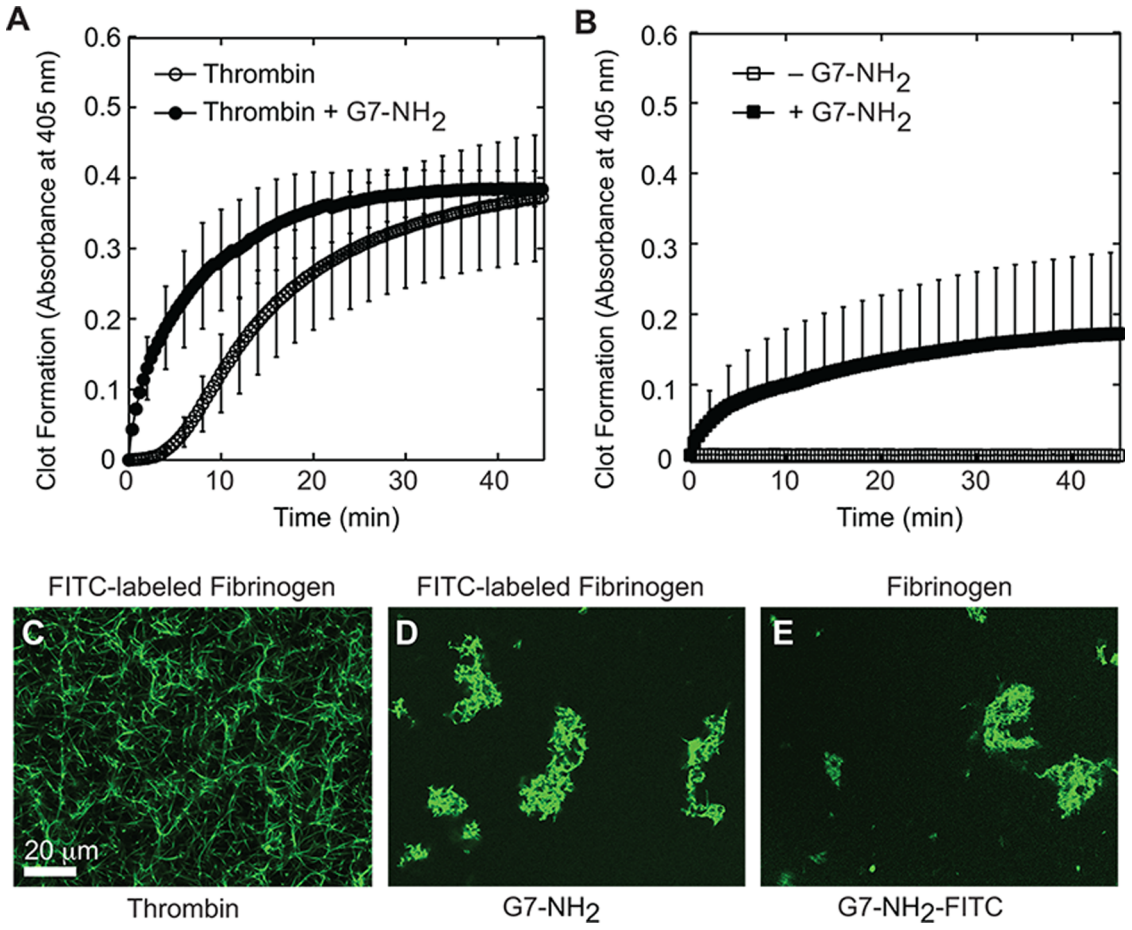

Figure 2. Cationic dendrimers induce fibrinogen aggregates. Clot formation was initiated by the addition of thrombin (2 nM, final) to fibrinogen (2 mg/mL, final) and monitored by changes in turbidity at 405 nm. In some experiments, G7-NH_2 PAMAM dendrimers (100 μg/mL, final) were added to the reaction immediately prior to thrombin addition (A). To test the effect of dendrimer directly on fibrinogen, fibrinogen with or without G7-NH_2 was monitored at 405 nm for changes in turbidity (B). Fibrin clot morphology was assessed by adding FITC-labeled fibrinogen to reactions described above. The resulting structure was then examined by laser-scanning confocal microscopy. Fibrin morphology in reactions containing FITC-labeled fibrinogen without G7-NH_2 (C), FITC-labeled fibrinogen with G7-NH_2 (D), and unlabeled fibrinogen with FITC-G7-NH_2 (E).

and thrombin's ability to cleave a chromogenic substrate was examined. As depicted in Figure 1B, cationic dendrimers do not interfere with thrombin's ability to cleave a chromogenic substrate, suggesting that thrombin's active site is unaffected by dendrimers and remains capable of cleaving fibrinogen; therefore, we decided to examine how cationic dendrimer affected fibrin formation in a purified system, where thrombin is not generated. A typical clotting response was observed for fibrinogen with the addition of thrombin, including a brief initial lag phase followed by rapid clot formation that plateaued at >45 min (Figure 2A). Upon addition of cationic dendrimer to the thrombin—fibrinogen system, the lag phase was eliminated and the rate of fibrin formation accelerated, reaching a plateau in only 30 min (Figure 2A). Notably, the presence of dendrimer did not significantly alter the peak optical absorbance attained, suggesting a similar extent of fibrin formation in the presence of dendrimer as compared to thrombin alone. Since our previous results suggested that thrombin generated was blunted in the presence of dendrimer,[13] but fibrin clot formation still occurred (Figure 1A), we examined the effect of cationic dendrimer upon fibrinogen alone, without thrombin. Cationic dendrimer addition to fibrinogen alone produced a clotting response with no lag phase and a rapid initial growth phase (Figure 2B) similar to dendrimer addition to the thrombin—fibrinogen reaction just discussed. These results demonstrate a rapid and direct (thrombin-independent) interaction between cationic dendrimer and fibrinogen. Moreover, the absence of a lag time following dendrimer addition argues for the nearly immediate formation of molecular associations between dendrimer and fibrinogen that occur in the absence of molecular cleavage. Importantly, the direct and immediate dendrimer–fibrinogen association and clot-like behavior demonstrated herein offer a compelling explanation for the immediate coagulopathy observed in all *in vivo* intravenous assessments of cationic high-generation dendrimers to date.

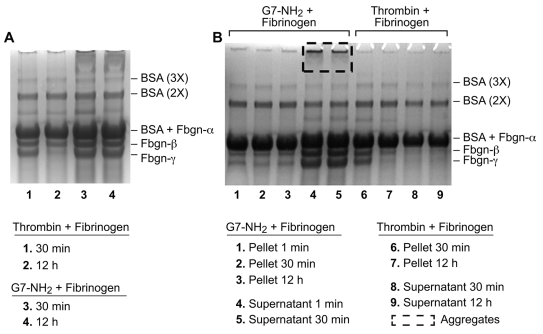

Figure 3. G7-NH_2 PAMAM dendrimers form high molecular weight aggregates with fibrinogen and albumin. Thrombin cleavage of fibrinogen results in no HMW aggregates (lanes 1 and 2), while addition of G7-NH_2 dendrimers immediately (lane 3) forms HMW aggregates, which are still visible 12 h after addition (lane 4) (A). HMW aggregates are seen only in the supernatant of fibrinogen and G7-NH_2 dendrimers (lanes 4 and 5) and are not in the pellet (lanes 1−3). HMW aggregates are not seen when thrombin and fibrinogen are incubated with each other (lanes 6−9) (B). HMW albumin aggregates are seen only in the presence of G7-NH_2 dendrimers (A, B).

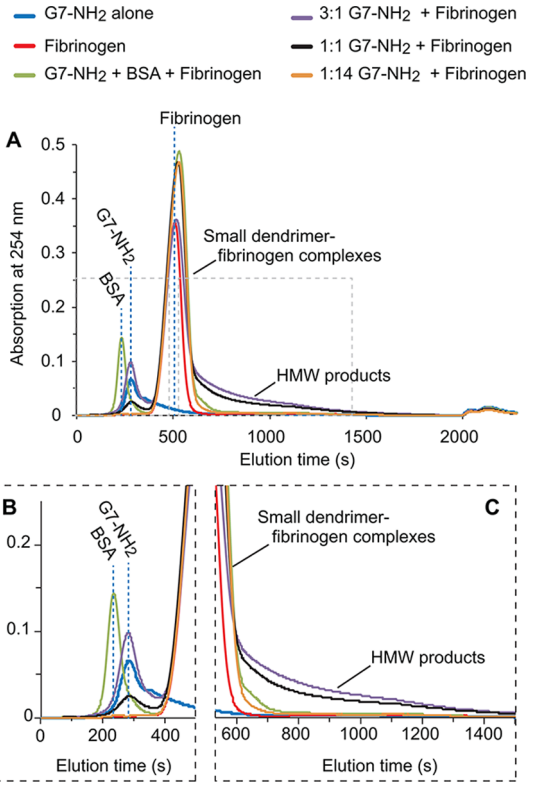

Figure 4. Cationic dendrimers induce high molecular weight fibrinogen aggregates. G7-NH_2 (blue) and fibrinogen (red) samples each provided a clean monomeric elution peak. Addition of dendrimer to fibrinogen produced a broadening of the fibrinogen peak (compare red *vs* orange) and substantial growth of the peak tail with increasing dendrimer/fibriongen molar ratio (compare orange to black to purple) (A). Insets of elution times between 0 and 500 s (B) and 600−1500 s (C) are included to better display dendrimer and product peak tails, respectively.

Microscopy of FITC-labeled fibrinogen was undertaken to characterize the product of this unusual thrombin-independent coagulation response and to visualize the dendrimer-induced perturbations on clot morphology. In the absence of cationic dendrimer, thrombin cleaves fibrinogen to form fibrin. Fibrin monomers polymerize to form protofibrils in one dimension, which then associate to produce a regular, but random, homogeneous mesh or network of fibrin (Figure 2C). In contrast, dendrimer treatment of FITC-labeled fibrinogen produced irregularly shaped, consolidated fibrinogen masses that appear to possess neither protofibrils nor defined secondary structure (Figure 2D). Additionally, separate imaging of clots with a FITC-labeled cationic dendrimer component showed dendrimer-based labeling throughout clots of unlabeled fibrinogen (Figure 2E). These results reveal pervasive dendrimer incorporation within each clot-like body and suggest the dendrimer-centric aggregation of fibrinogen, further strengthening the idea that dendrimer−fibrinogen associations underlie the DIC-like conditions observed *in vivo*. Notably, there is no evidence of fibrinogen cleavage to fibrin with dendrimer exposure (*e.g.*, fibrinopeptide cleavage), thus supporting a surrogate mechanism for this key coagulation event, independent of thrombin.

SDS-PAGE gel analysis was performed to assess the molecular products formed by dendrimer treatment of fibrinogen. Digested products of dendrimer−fibrinogen reactions were compared to thrombin-treated (positive) and untreated (negative) controls (Figure 3). Thrombin treatment of fibrinogen demonstrated a time-dependent loss of the smallest fibrinogen band, just below 50 kDa (Figure 3A, lanes 1 and 2), resulting from covalent gamma-chain cross-linking mediated by residual plasma transglutaminase (FXIIIa) in the thrombin stock, as has been shown.[15] With reaction time, these gamma-chain dimers grow to multimers that are increasingly resistant to cleavage.[15] This cleavage-mediated cross-linking was not observed following dendrimer treatment (Figure 3A, lanes 3 and 4; 3B, lanes 4 and 5). However, in addition to fibrinogen fragment bands that were similar to the untreated control, cationic dendrimer treatment of fibrinogen produced very high molecular weight (HMW) products that ran only slightly in the gel and spanned the area from the well to the faint band of residual (unreduced) fibrinogen near 340 kDa. Such HMW entities were observed in all dendrimer-treated samples, but were not observed in any other samples or controls. Moreover, PAGE banding patterns for

TABLE 1. AsFlFFF Peak Integrations (dendrimer−FBG[a] peak and tail ratios)

treatment condition	FBG peak area	FBG tail area	tail (% of total)
3:1 G7/FBG	31.69	12.63	40
1:1 G7/FBG	33.89	9.99	29
1:14 G7/FBG	26.00	2.64	10
FBG only	32.84	1.41	9

[a] Fibrinogen.

dendrimer-treated fibrinogen were similar for all time points, including 1 min, 30 min, and 12 h treatment periods (Figure 3B, lanes 1–5), demonstrating the extremely rapid formation of dendrimer–fibrinogen associations that appear to remodel very little over time. Notably, when fibrinogen was treated initially with thrombin followed by cationic dendrimer, formation of HMW products was not observed (data not shown). These results strongly suggest dendrimer-mediated aggregation of fibrinogen that is dependent upon the presence of uncleaved fibrinogen and distinct from thrombin proteolysis of fibrinogen. Interestingly, similar HMW products were observed in PAGE analysis of cationic dendrimer-treated single-protein samples of bovine serum albumin (BSA) alone (data not shown). However, unlike fibrinogen products, fractions of HMW products in BSA–dendrimer samples increased with duration of exposure to cationic dendrimer.

In sharp contrast to the foregoing PAGE results, reaction of cationic dendrimer with protamine, a small, highly cationic blood protein (5–10 kDa) composed of roughly 60% arginine, did not produce any perceptible amount of interaction product or aggregation (Supplemental Figure 1). Conversely, the reaction of anionic (generation-7 carboxylate-terminated) dendrimer with protamine (2 mg/mL) resulted in strong HMW bands that diminished with decreasing G7-COO^-/protamine molar ratios from 1:113 to 1:4760, where they vanished (data not shown). (These molar ratios were intended to bracket and include the estimated 1:340 molar ratio needed to form a complete protamine monolayer on a G7-dendrimer surface.) Together, these fibrinogen–, albumin–, and protamine–dendrimer product results demonstrate electrostatically mediated dendrimer interactions with oppositely charged proteins to produce fibrinogen/albumin HMW aggregates distinct from thrombin-mediated fibrin polymerization products.

Since cationic dendrimers alone do not electrophorese (data not shown), aggregate product sizing by electrophoresis alone was uncertain due to the potential for exposed dendrimer surface charge density in the HMW products to greatly affect product movement within the gel. Thus, to monitor the effect of dendrimer charge density and confirm and characterize the dendrimer and fibrinogen interaction products, asymmetrical flow field-flow fractionation (AsFlFFF) was employed for aggregate particle hydrodynamic size-based separation. Clean monomeric peaks were obtained for BSA (data not shown), dendrimer, and fibrinogen alone at 3.9, 4.7, and 8.5 min retention times, respectively (Figure 4A, B). With dendrimer treatment (1:14 G7-NH_2/fibrinogen ratio), the dendrimer peak vanished and the fibrinogen peak broadened, and the elution time shifted slightly from 8.2 to 8.7 min (Figure 4A, C, red *vs* orange curves). Increasing the dendrimer:fibrinogen molar ratio from 1:14 to 3:1 resulted in the appearance of a free dendrimer peak

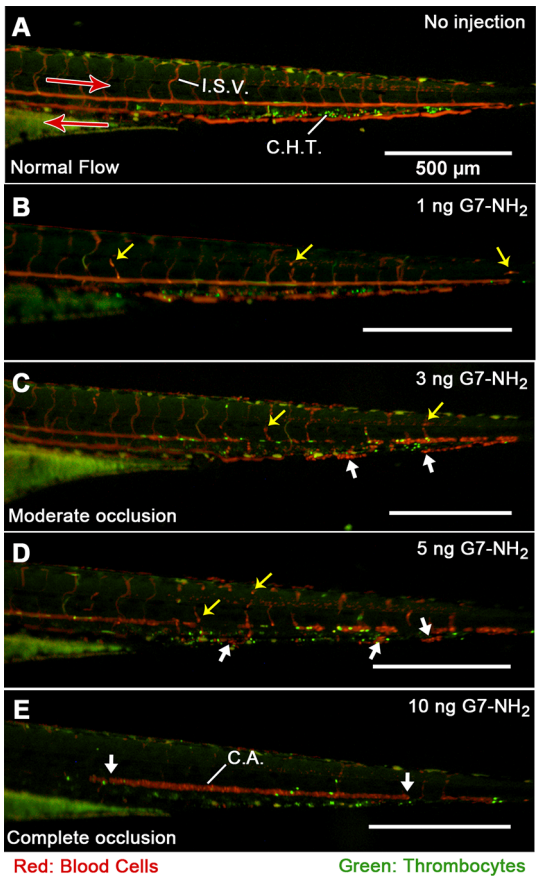

Figure 5. Dose-dependent G7-NH_2 occlusion in zebrafish embryos 1 min postinjection. ZFEs (4dpf gata-1::dsred/CD-41::EGFP) were anesthetized, mounted, injected, and imaged as described in Methods. The top panel (A) depicts unperturbed caudal blood flow as streaks of red and green light visible in the major caudal artery (CA, left to right), vein (right to left), and intersegmental vessels (ISV). Punctate green and red spots in between the major caudal artery and vein indicate the location of the caudal hematopoietic tissue (CHT). Subsequent images (proceeding downward (B–E), with increasing G7-NH_2 dose) depict increased cellular adhesion and vascular occlusion resulting from dendrimer injection, culminating in no visible blood flow following an injection of 10 ng of G7-NH_2. The yellow arrows depict individual red blood cells trapped inside the vessel, while the large white arrows show significant blood clots inside the vessels. Notice in (E) the caudal artery is completely occluded with no observable flow in the major caudal vein.

along with corresponding growth in area and length for the tail of the fibrinogen product peak (Figure 4A, C). Significantly, with dendrimer treatment, the fibrinogen peak gained a tail that increased in area from 10% to 40% of the total peak area by increasing dendrimer/fibrinogen ratios from 1:14 to 3:1 (Table 1). Moreover, this tail extended to 16 min beyond the fibrinogen peak for the 3:1 dendrimer/fibrinogen sample. Given the size-based separation inherent in the AsFlFFF technique, these results in dendrimer-treated fibrinogen samples indicate a continuum of aggregate sizes ranging from simple (possibly 1:1) dendrimer–fibrinogen associations (indicated by the large product peak with a small shift in retention time from the fibrinogen-only peak) to

progressively larger aggregates, evinced most clearly by the protracted peak tail for the 3:1 dendrimer/fibrinogen sample.

The preceding data strongly suggest rapid dendrimer-mediated aggregation of fibrinogen and provide data consistent with products of such interactions, with evidence for an electrostatic mechanism extending to many negatively charged blood components. Consequently, direct observation of *in vivo* coagulopathy was sought in the transparent zebrafish embryo model of blood coagulation to visualize the extent, character, and time dependence of the *in vivo* DIC-like condition arising from cationic dendrimer interaction in blood.[14] Hybrid CD-41::EGFP/gata-1::dsred 4dpf ZFEs, utilized for fluorescence-facilitated visualization of RBCs and thrombocytes in the circulation, were anesthetized, mounted, and injected with dendrimer preparations of various doses. Cationic dendrimer injections into ZFEs were observed to produce immediate coagulation at the injection site that rapidly resulted in caudal (tail) vessel occlusions that scaled roughly with cationic dendrimer dose (Figure 5B–E, supplemental video 1). In separate experiments, FITC-labeled cationic dendrimer injections into wild-type (AB) nonfluorescent ZFE produced fluorescently labeled clots along with diffuse staining throughout the vasculature, indicating cationic dendrimer association with the vascular endothelium (Supplemental Figure 2). This suggests that cationic dendrimers participate directly in the observed *in vivo* DIC-like events in blood and that cationic dendrimers may possess a high affinity for platelets and endothelial cells or may bind vascular endothelium, either directly or together with complexed plasma proteins. Additionally, identically administered anionic and neutral G6.5/G7 dendrimers produced no observable vascular occlusion (data not shown). This is consistent with both previous *in vivo* (rodent) observations that neutral and anionic dendrimer dosing was limited only by dendrimer solubility and not toxicity[14] and also recent *in vitro* findings demonstrating that neutral and anionic dendrimer functionalizations are minimally activating toward platelets *in vitro* (little/no platelet aggregation, morphology change, or granular release).[8,13] Functional equivalence has been previously established for zebrafish coagulation machinery in comparison to human blood.[16–18] Moreover, zebrafish blood and platelets are responsive to a variety of procoagulants and platelet agonists (*i.e.*, ristocetin, collagen, rabbit brain thromboplastin, Russell's viper venom, thrombin, adenosine diphosphate, and arachidonic acid), anticoagulants (*i.e.*, heparin, hirudin, sodium citrate, and warfarin), and antiplatelet agents (*i.e.*, acetylsalicylic acid (aspirin), abciximab, and aurin tricarboxylic acid).[19–23] Thus, a variety of anticoagulant and antiplatelet agents were applied prophylactically to ZFE to elucidate the mechanism of dendrimer-induced coagulopathy. However, none of these embryo pretreatments (administered 30 min or 2 h before dendrimer injection) prevented or noticeably diminished the occlusion resulting from a subsequent cationic dendrimer injection (3 ng, Supplemental Figure 3 and data not shown), but bleeding complications were common at the dendrimer injection site in ZFE pretreated/preinjected with warfarin, sodium citrate, lepirudin, or heparin (data not shown). Prophylactic treatments included the following agents (with maximum concentrations stated): pretreatment with warfarin (500 μM, final), sodium citrate (0.38%, final), or acetylsalicylic acid (75 μg/mL, final); preinjection (1 nL) with abciximab (42 μM), lepirudin (145 484 U/mL), or heparin sulfate (15 mg/mL) (Supplemental Figure 3). Importantly, pretreatment of ZFE by soaking in sodium citrate for 2 h (0.38%, final) was observed to block the coagulogenic action of injected human thrombin (1 nL, 3 μM), although this was only observed in roughly half of embryos tested (supplemental videos 2 and 3). The source of this inconsistency is unknown, but may be attributable to genetic variation of wild-type ZFE and nonhomology between zebrafish and human thrombin.[24]

DISCUSSION

Dose- and generation-dependent toxicity for cationic dendrimers in a variety of cell types and experimental systems has been reported (reviewed elsewhere[25]). Specifically, decreasing toxicity has been observed for decreasing dendrimer generation with higher maximum tolerated doses for lower generation dendrimers than for higher generation cationic dendrimers.[25] Previous reports of hemolysis,[14,26] platelet activation *in vitro*,[13] and fibrin degradation products in the blood of G4-NH_2 and G7-NH_2 dendrimer-injected rodents[14] consistently suggest a strong procoagulant role for cationic dendrimers in blood. Notably, these results also observed dose- and generation-dependent blood toxicity with G3 and G4 generation dendrimers.[8,13,25] Previous studies by our laboratory as well as other groups have focused on the effect of high-generation dendrimers on platelet function, but their effects on soluble coagulation proteins have been inadequately studied to date.[8,13,25] Significant platelet activation usually results in exposure of phosphatidylserine and platelet-dependent thrombin generation, but administration of cationic G7 dendrimers to plasma paradoxically inhibited thrombin generation.[13] In addition, G7-NH_2 dendrimers blunted fibrin clot formation (Figure 1A). Collectively, these findings set up an apparent *in vitro–in vivo* dichotomy of response to cationic dendrimers where the dendrimer architecture (G7) that produces the most thrombotic response has also been observed to inhibit production of the most critical coagulation enzyme, thrombin. Significantly, this dichotomy is not explainable as a simple dendrimer-mediated deactivation or binding of thrombin since thrombin retains its enzymatic activity in the presence of cationic dendrimers (Figure 1B). Thus, cationic

dendrimer attenuation of thrombin and clotting is likely to occur at the level of thrombin generation, and not thrombin activity.

Given the severe coagulopathy observed *in vivo*, the observed *in vitro* inhibition of thrombin generation (without inhibition of thrombin activity) presents an interesting potential distinction between the thrombotic actions of cationic dendrimer and thrombin resulting from competing molecular interactions with cationic dendrimer. In this respect, the simplified coagulation assay comprising only thrombin and fibrinogen demonstrated that cationic dendrimers actually accelerate clot formation and remove the lag phase observed for this simplified thrombin-clotted fibrinogen condition (Figure 2A). Further simplification of the assay demonstrated that fibrinogen clotting proceeds immediately following dendrimer addition (*i.e.*, no lag phase) (Figure 2B), producing dense, consolidated clots with pervasive dendrimer staining (Figure 2D, E) *even in the absence of thrombin*. The apparent contradiction between these accelerated clotting results and the attenuation of clotting in PPP with dendrimer exposure (Figure 1A) strongly suggests the influence of additional, competing interactions of cationic dendrimer with many of the cogulation-naïve plasma proteins present in PPP, but not present in these simplified binary or ternary coagulation assays (Figure 2).

Prior work has demonstrated interactions between cationic dendrimers and plasma proteins[27−29] to the extent that hemolysis of purified red blood cells is blunted in the presence of added human serum albumin,[30] demonstrating that both platelets and red blood cells are partially protected by the protein-rich environment of whole blood. Notably, despite previous *in vitro* analysis of dendrimer-induced platelet activation,[13] including extensive adhesion, aggregation, and proinflammatory secretions, extensive hemolysis and platelet activation have not been demonstrated *in vivo* following cationic dendrimer injection, even amidst extensive coagulopathy. Significantly, this is the first report of HMW products arising from protein−dendrimer interactions and strongly suggests that the previously reported DIC-like phenomenon may arise, in part, from dendrimer interactions with proteinaceous coagulation zymogens.

This thrombin- and (possibly) fibrin-independent interaction of cationic dendrimers with fibrinogen may simply be based on electrostatic interactions. Soluble fibrinogen (uncleaved) at physiological pH possesses a net −20 anionic charge with significant localized negative charge density on the E region (−8), which becomes positively charged (+5) upon cleavage of the fibrinopeptides to form insoluble fibrin (−7 charge overall). Thus, dendrimer−fibrinogen electrostatic interactions may be more favorable than dendrimer−fibrin interactions. This assessment is borne out in SDS-PAGE results (Figure 3) demonstrating that cationic dendrimer treatment of fibrinogen produced aggregates of otherwise unmodified fibrinogen. This was supported by the SDS-PAGE gel presence of HMW products that exceeded the size of unreduced fibrinogen (340 kDa) and, in some cases, that did not leave the loading well. These products were not present following dendrimer treatment of thrombin-activated fibrinogen (data not shown). Additionally, the similarity of dendrimer-treated fibrinogen fragment bands to the untreated fragment band patterns (*i.e.*, negative control) demonstrates an absence of the fibrinogen cleavage and cross-linking that are evident in thrombin-treated controls. Thus, dendrimer−fibrinogen molecular aggregates are proposed to form from strong electrostatic interactions between densely charged (positive) dendrimer surfaces and the oppositely charged (negative) D or E domains of uncleaved fibrinogen. Such aggregates would effectively comprise quasi dimers, trimers, and multimers of fibrinogen formed by electrostatic association between fibrinogen and cationic dendrimers. Given the numerous binding sites available on G7 dendrimers with 512 surface primary amines per molecule, such electrostatic binding of multiple fibrinogen molecules would be limited only by packing parameters and steric hindrance between adjacent fibrinogen molecules. However, since fibrinogen is roughly the size of four or five dendrimers placed end to end (9 × 45 nm long rod *vs* a 8.1 nm diameter sphere, respectively) and the negative regions of the D and E fibrinogen domains are present on opposite molecular faces, one fibrinogen molecule may interact with more than one dendrimer molecule, enhancing aggregate stabilization by charge−charge multimer cross-linking.

The AsFlFFF data demonstrate that most products formed by dendrimer−plasma protein complexes are likely simple 1:1 dendrimer−fibrinogen associations, but additionally confirm that much larger aggregates are also formed, particularly if provided dendrimer excess bias in the binary solution composition. These larger entities likely include additional dendrimers electrostatically adsorbed onto the original dendrimer−fibrinogen core, perhaps forming progressively larger multimer aggregates with alternating dendrimer−fibrinogen structure. This could occur with primary dendrimer−fibrinogen associations forming between the densely anionic E domain at fibrinogen centers and densely cationic dendrimer surfaces, and weaker, secondary associations forming between additional dendrimers and the somewhat less densely anionic D domains at the ends of the fibrinogen molecule on the opposite face from the E region charges. Further, the area relationship of the AsFlFFF product elution peak to its tail (Table 1) provides an estimated number-based proportion of small, primary aggregates relative to larger, more complex aggregate compositions. The tail's proportion to the total peak area increases with increasing dendrimer feed ratios, demonstrating the requirement for excess dendrimer for the generation of

larger FFF aggregates. The smooth decay of the product tail with increasing aggregate size demonstrates that no single binding combination is energetically most favorable beyond the major peak. Rather, the size distribution of larger aggregation products seems to be based on statistical probabilities of forming aggregates of given sizes based on alternating dendrimer–fibrinogen interactions with decreasing probability for each successive unit addition.

The most pronounced aggregate presence in gel electrophoresis results (Figure 3) was observed for dendrimer-treated samples of fibrinogen and BSA together, and the presence of BSA adds a shoulder to the dendrimer–fibrinogen product peak in the AsFlFFF results (Figure 4). BSA carries net charges of −10 and −8 on two of its three domains at neutral pH,[31] has a pH-regulating function in the blood,[32] and is highly predisposed to adsorption to foreign bodies in contact with blood.[33] At 2–3 and 40–45 mg/mL in human blood, respectively, fibrinogen and albumin together represent a substantial mass fraction of total soluble blood protein content (70 mg/mL total). They also represent two very different protein components in blood, with their drastically differing glycosylation patterns, shape (rodlike *vs* globular), structure and composition (many domains and fragments *vs* single globular strand), and function (hemostasis *vs* pH regulation and fatty acid transport). One major commonality shared by these two very disparate plasma proteins is a high negative charge density on two of their respective domains. That this property elicits electrostatically based dendrimer–fibrinogen and dendrimer–albumin interactions is seemingly confirmed by the absence of dendrimer aggregation with a densely cationic blood protein, protamine. Further, it reveals the potential for extensive "nonspecific" dendrimer-induced electrostatic protein aggregation extending well beyond a fibrinogen-only coagulation-specific response to include many blood proteins with negatively charged regions. Given up to 10 000 known proteins and 15 000 isoforms in the human plasma proteome,[34–36] most with anionic glycosylation patterns and acidic pI values,[37] there is substantial potential for cationic dendrimer–protein electrostatic interactions in whole blood. This electrostatic mechanism of aggregation is further supported by the charge-dependency demonstrated in a previous report of increased platelet aggregation observed both for increased cationic dendrimer generation and for increased intrageneration surface charge.[8] *In vivo*, such charge-based proteinaceous aggregation phenomena could rapidly produce numerous microemboli capable of adhesion to the endothelium, with subsequent consolidation into occlusions and microvasculature infarcts.

Thus, cationic G7 dendrimers are proposed to exhibit very unusual thrombogenic behaviors through strong, charge–charge interactions with a variety of many different blood components, and perhaps no one blood element preferentially. Additionally, the capacity of cationic G7 dendrimers to bind both platelets[13] and fibrinogen may also explain previous observations of platelet aggregation and adhesion to fibrinogen, each in the presence of abciximab, the platelet $\alpha_{IIb}ß_3$ (platelet fibrinogen receptor) agonist.[13] Ultimately, as an alternative to the classic enzymatic mechanism of blood coagulation, high-generation dendrimers may provide an unconventional "coagulation" mechanism consisting of complex, multicomponent interactions between platelets, dendrimers, fibrinogen, and many other anionic blood proteins. In this manner, rapid, nonspecific aggregation events could consume significant amounts of platelets and fibrinogen, as well as other negatively charged cellular and molecular elements of blood, forming aggregates and microemboli that are then consolidated by both flow and microvascular transport dynamics into massive occlusions. While the focus of the current study has been on cationic G7 dendrimers, lower generation dendrimers should also be examined carefully for similar protein aggregation properties since previous reports have demonstrated that G3 dendrimers can induce platelet activation and blood toxicity has been observed with G4 generations.[8,13,25]

These dynamics are evident in dose–response relationships observed *in vivo*. In a dendrimer-poor scenario in which DIC-like aggregation is limited by cationic G7 dendrimer concentration, dendrimer addition results in the formation of comparatively smaller aggregation products (Figure 4) and may thus result in only a minimal amount of thrombosis and vascular occlusion. This outcome was observed for the lowest doses of cationic G7 dendrimer injected into ZFE (≤1 ng) and the rodent dendrimer doses (G4- and G7-NH_2) at which some rodents survived (5–10 mg/kg).[14] Alternatively, when the dendrimer dose is comparatively and sufficiently higher, the majority of platelets and fibrinogen are consumed[13,14] by extensive aggregation that may also include significant fractions of other blood proteins (Figure 4), leading to widespread coagulopathy *in vivo*.[14] Such an extensive thrombogenic response to high-generation cationic dendrimer doses was observed *in vivo* as the total cessation of intravascular blood flow in ZFEs following the highest cationic dendrimer dose injected intravenously (10 ng, Figure 5E, supplemental video 1) and the rapid mortality of rodent subjects receiving nontolerated dendrimer intravenous doses (G4-, G7-NH_2 >10 mg/kg).[14]

Since these present *in vivo* results represent the first usage of ZFEs for assessments of procoagulant nanomaterials in blood, it is important to underscore that the components and processes of zebrafish coagulation are well-studied and have been established as functionally equivalent to their human counterparts.[16–18] Moreover, zebrafish blood and platelets are responsive to a variety of procoagulants and platelet agonists in addition to many anticoagulants and antiplatelet agents.[19–23] The

conservation of these inhibitory effects was exemplified in the prevention of human thrombin-induced clotting in some ZFEs by prophylactic treatment (see supplemental videos 2 and 3) and separate observations of increased bleeding from the dendrimer injection site in prophylactically anticoagulant/antiplatelet-treated ZFEs (data not shown), specifically those previously presoaked/preinjected with warfarin, sodium citrate, heparin, or lepirudin. In the present context, the observation that none of the inhibitors examined affected the observed dendrimer-mediated coagulopathy confirms that the dendrimers' influences on coagulation are independent of classical procoagulant mechanisms. These findings also demonstrate the utility of the ZFEs for real-time visualization and description of nanomaterial effects in blood.

CONCLUSIONS

The findings presented here describe rapid and extensive aggregation of fibrinogen and other anionic blood proteins by densely charged cationic G7 dendrimers, observed to produce HMW aggregate species by a thrombin-independent and cellular activation-free mechanism. These effects were not inhibited by any of a wide array of antithrombotic or antiplatelet agents *in vivo*. The acidic natures and high concentrations of many endogenous proteins in blood (70 mg/mL total, 2.5 mg/mL fibrinogen and 45 mg/mL albumin, respectively) predispose these blood elements to this type of rapid and extensive aggregation with G7 dendrimers having uniquely dense cationic surfaces (*i.e.*, 512 tightly packed primary amine cations per G7 dendrimer under physiological conditions). Thus, cationic G7 dendrimer architecture may provide a rare cation presentation, unshared by any linear polycations, that provides potential for more potent, stable, dendrimer-mediated electrostatic aggregation of human plasma proteins as demonstrated here for fibrinogen and BSA. This is proposed as the likely basis for adverse reactions to intravenous cationic dendrimer injection observed *in vivo* in rodents[14] and ZFEs. These findings underscore existing concerns for intravenous applications of cationic G7 dendrimers and provide a warning for their biological applications to be designed with extreme caution and careful attention to their reactivity in blood. Future studies should examine the dose-, generation-, and surface group density-dependency for these clot-like and cellular activation effects of cationic dendrimers to identify those dendrimer doses and architectures that are safe for intravenous administration.

METHODS

Materials and Reagents. G6.5-COOH and G7-NH_2 poly(amido amine) dendrimers (Sigma Aldrich, USA) were purified by preparative size-exclusion chromatography and characterized as previously described.[14] The fibrinogen clot microscopy experiments utilized fluorescein isothiocyanate-conjugated G7-NH_2 (G7-NH_2-FITC) dendrimers whose labeling, purification, and characterization was described previously.[7,13] All dendrimers were lyophilized following their purification and subsequently diluted in endotoxin-free water or phosphate-buffered saline (pH 7.4) prior to their use. Human fibronectin-free fibrinogen (Enzyme Research Lab), bovine serum albumin (fraction V, EMD Chemicals, Inc.); ethylenediaminetetraacetic acid (EDTA, 0.5 M, Gibco); human thrombin (2500 nM) and heparin (sodium salt, bovine intestinal mucosa, Sigma); sodium citrate dehydrate (Fisher Scientific); abciximab (42 μM) and lepirudin (145484 U/mL) (Hospital Pharmacy, University of Utah, Salt Lake City, USA); endotoxin-free water (Lonza); acetylsalicylic acid (gift of Dr. C. Terry, University of Utah, Salt Lake City, USA); and protamine (gift of Dr. Sivaprasad Sukavaneshvar, Thrombodyne Inc., Salt Lake City, USA) were all used as received.

Whole Blood Collection and Plasma Preparation. This study was performed as approved by the University of Utah Institutional Review Board, and all subjects provided informed consent. Human peripheral venous blood (25−50 mL) was collected into acid-citrate-dextrose (1.4 mL ACD/8.6 mL blood) from healthy, medication-free, fasting adult subjects as previously described.[13] Plasma was harvested by centrifuging whole blood at 500*g* for 20 min and then once more at 13000*g* for 2 min to remove any remaining cell contaminants to yield platelet-poor plasma.

Zebrafish Embryos. Zebrafish aquaculture has been described elsewhere.[38] Breeding colonies were maintained by the University of Utah Zebrafish Core Facility on a 14 h light/10 h dark light cycle. ZFEs were obtained from fluorescent transgenic (Tg) zebrafish, either the recombinant Tg(CD-41::EGFP) variant possessing either green fluorescent protein (EGFP)-expressing thrombocytes and thrombocyte precursors (CD-41 promoter region)[18] or hybrid Tg(CD-41::EGFP/gata-1::dsred), red fluorescent protein (dsred)-expressing red blood cells (gata-1 promoter region),[39] and EGFP-thrombocytes. For clarity, transgenic lines will hereafter be referred to without their Tg(xxxx::xxxx) nomenclature. Embryos were incubated at 28.5 °C in E3 media (aqueous 5 mM NaCl, 0.17 mM KCl, 0.4 mM $CaCl_2$, 0.16 mM $MgSO_4$) supplemented with 0.000 016% methylene blue (antifungal).

Zebrafish Embryo Injection and Imaging. All procedures were performed according to an established IACUC-approved protocol. Either CD-41::EGFP or gata-1::dsred/CD-41::EGFP ZFE, at 3-, 4-, or 6-day-postfertilization (dpf), were sorted, anesthetized topically with tricaine methanesulfonate MS222 (tricaine), and immobilized in low-melt agarose (1% in sterile water without tricaine) maintained at 42 °C, as described previously.[38] Human thrombin or PAMAM G7-NH_2 dendrimers in sterile phosphate-buffered saline (PBS) were injected (1 nL) intravenously into the venous blood flow dorsal from and immediately proximal to the heart of 3 or 6 dpf ZFEs using a YOU-1 micromanipulator (Narishige), MPPI-3 microinjector (ASI), and BP-15 backpressure unit (ASI) for injection control and a M80 Leica stereomicroscope for visualization during the injection. Injected ZFEs were quickly transferred to an upright Nikon Eclipse 600 fluorescent microscope and imaged using a CRI Nuance multispectral imaging system model N-MSI-420-FL controlled by IPL software. Alternatively, ZFEs were both injected and imaged on a Leica M165 FC microscope, and images were captured using 5.5 megapixel CCD controlled by Leica image software, LAS v4.0. For time-lapse microscopy, embryo blood flow and coagulation images were captured at a rate of 3 images per second. Single still-frame images were taken at longer shutter times (>200 ms) to offer movement-based contrast between circulating and adherent blood cells/thrombocytes. Images demonstrating FITC−dendrimer localization were obtained following injection of FITC-labeled dendrimers into wild-type ZFEs. Images of extent of vascular occlusion were obtained following injection of unlabeled dendrimers into CD-41::EGFP or gata-1::dsred/CD-41::EGFP ZFEs, respectively.

In some experiments, ZFEs were pretreated before dendrimer treatment with an anticoagulant or antiplatelet agent by direct soaking for at least 30 min and up to 12 h (before dendrimer injection) in E3 embryo media-based solutions of warfarin (500 μM, final), acetylsalicylic acid (75 μg/mL, final), or sodium citrate (0.38%, final). Such small-molecule agents have previously been demonstrated to freely diffuse into ZFEs.[20,22] In other treatments, zebrafish were pretreated with injections (1 nL) of abciximab (42 μM), lepirudin (145484 U/ml), or heparin sulfate (15 mg/mL) in sterile PBS 2 h before dendrimer injection. In other experiments, treatments occurred immediately or 30 min before dendrimer injection. Timing of drug treatments had no effect.

Thrombin Activity Assay. Thrombin activity was measured as previously described[40,41] with the notable exception that dendrimer (100 μg/mL, final) was added to the reaction. The activity of the enzyme was measured by light absorbance at 405 nm on a Spectramax VMAX plate reader (Molecular Devices).

Clotting Assays. Clot formation was initiated by addition of recombinant tissue factor (Innovin (1:10 000, final)) and $CaCl_2$ (20 mM, final) to platelet-poor plasma in the presence or absence of dendrimer (100 μg/mL, final), and clot formation was monitored by changes in light absorbance at 405 nm on a Spectramax VMAX plate reader (Molecular Devices). To examine the effect of dendrimers on only fibrinogen polymerization, thrombin (2 nM, final) and dendrimer (100 μg/mL, final) were added to purified human fibrinogen (2 mg/mL, final) in PBS (pH 7.4) supplemented with $CaCl_2$ (3 mM) and clot formation was monitored. In separate experiments, thrombin was excluded from the sample preparation to assess dendrimer-mediated clot formation in the absence of thrombin.

Clot Morphology Assessment. Clot formation and imaging were performed as described previously.[40] Briefly, clots were produced by incubating AlexaFluor-488-labeled fibrinogen (10 μg/150 μL sample, 3.2% of total fibrinogen) with $CaCl_2$ (5 mM final) and either thrombin (2 nM final) or G7-NH_2 dendrimer (100 μg/mL final) for 30 min. Confocal microscopy was accomplished using a FV300 1 $\times$ 81 microscope and FluoView software (Olympus, Center Valley, USA, Fluorescent Microscopy Core Facility, University of Utah). Both 20$\times$ and 60$\times$ objectives were used. Optical sections were collected at randomly chosen locations.

SDS-PAGE of Protein–Dendrimer Products. Purified human fibrinogen (2 mg/mL final) in 140 mM PBS supplemented with $CaCl_2$ (3 mM final) and bovine serum albumin (1 mg/mL final) was reacted with dendrimer (100 μg/mL final) or purified human thrombin (5 nM final). After reaction times of 1 min, 30 min, 2 h, 12 h, or 72 h, EDTA (20 mM, final) was added. In some experiments, clots and supernatants were separated by centrifugation (14000*g*, 4 min), and each sample fraction was digested in urea (6 M, final) and DTT (40 mM, final) with heating (60 °C, 1 h). Clot fractions did not digest completely in the case of thrombin treatment. Thus, in one experiment, centrifuged clot/pellet fractions were digested in 7.5 M urea and 40 mM DTT. Samples were mixed with loading dye, denatured, and separated on a 4–12% PAGE gel (Novex, USA) for 60–90 min. Gels were stained with Acqua Stain (Bulldog Bio, USA) for at least 20 min, and images were captured using a Molecular Imager Gel Doc XR System (Bio-Rad, USA).

Size-Based Separation of Fibrinogen–Dendrimer Reaction Products. Asymmetrical flow field-flow fractionation was employed to separate product(s) of dendrimer–fibrinogen interactions based on hydrodynamic size. G7-NH_2 dendrimer was added to fibrinogen (2 mg/mL, final) in PBS at dendrimer/fibrinogen molar ratios of 3:1, 1:1, or 1:14 and vortexed for about 5 s. In one treatment condition, dendrimer was reacted with fibrinogen (2 mg/mL, final) in PBS supplemented with $CaCl_2$ (3 mM, final) and BSA (1 mg/mL, final), as described above. Sample aliquots (20 μL) were manually injected into the FFF column (25 °C) and focused for 7 min in the mobile phase (PBS) with cross-flow (0.1 mL/min) to effect size-based particle separation. Samples were then eluted by a constant flow of 1 mL/min with a field flow of 2 mL/min for 2 min, followed by a power-decay gradient from 2 to 0.1 mL/min over 15 min, 0.1 mL/min for 10 min, and 0 mL/min for 13 min. A complete description of the instrument and relevant methodology has been reported previously.[42]

Statistical Analysis. Sample experimental replicates of at least $n = 3$ were collected from biological replicates of $n = 2$. Where applicable, pairwise comparisons were performed with a Student's t test with $p < 0.05$ considered significant.

Conflict of Interest: The authors declare no competing financial interest.

Acknowledgment. The authors gratefully acknowledge D. Lim for figure preparation. Financial support was provided by the NIH (RO1DE019050, RO1 HL066277-11, and 1U54HL112311-01), the American Heart Foundation (11POST7290019), the Utah Science Technology and Research (USTAR) initiative, a University of Utah Graduate Research Fellowship, and an Interdisciplinary Seed Grant from the University of Utah.

Supporting Information Available: Figures of SDS-PAGE analysis of protamine with cationic or anionic G7-PAMAM, vascular dendrimer distributions in ZFE following FITC-cationic dendrimer injection, and vascular occlusions in ZFE receiving warfarin or heparin prophylaxis (before dendrimer injection), videos of thrombin-induced ZFE thrombosis and its prevention by sodium citrate prophylaxis, and videos of G7-NH2 dose-dependent occlusion in zebrafish embryos. These materials are available free of charge *via* the Internet at http://pubs.acs.org.

REFERENCES AND NOTES

1. Clarke, S.; Tamang, S.; Reiss, P.; Dahan, M. A Simple and General Route for Monofunctionalization of Fluorescent and Magnetic Nanoparticles Using Peptides. *Nanotechnology* **2011**, *22*, 175103.
2. US Demand for Nanotechnology Medical Products to Approach $53 Billion in 2011, report. http://nanotechwire.com/news.asp?nid=4446 (accessed July 3, 2008).
3. Medina, S. H.; El-Sayed, M. E. Dendrimers as Carriers for Delivery of Chemotherapeutic Agents. *Chem. Rev.* **2009**, *109*, 3141–57.
4. Heath, J. R.; Davis, M. E. Nanotechnology and Cancer. *Annu. Rev. Med.* **2008**, *59*, 251–265.
5. Heath, J. R.; Davis, M. E.; Hood, L. Nanomedicine Targets Cancer. *Sci. Am.* **2009**, *300*, 44–51.
6. Frens, G. Controlled Nucleation for the Regulation of the Particle Size in Monodisperse Gold Suspensions. *Nat. Phys. Sci.* **1973**, *241*, 20–22.
7. Kitchens, K. M.; Kolhatkar, R. B.; Swaan, P. W.; Eddington, N. D.; Ghandehari, H. Transport of Poly(amidoamine) Dendrimers across Caco-2 Cell Monolayers: Influence of Size, Charge and Fluorescent Labeling. *Pharm. Res.* **2006**, *23*, 2818–2826.
8. Dobrovolskaia, M. A.; Patri, A. K.; Simak, J.; Hall, J. B.; Semberova, J.; De Paoli Lacerda, S. H.; McNeil, S. E. Nanoparticle Size and Surface Charge Determine Effects of PAMAM Dendrimers on Human Platelets *in Vitro*. *Mol. Pharm.* **2012**, *9*, 382–393.
9. Heiden, T. C.; Dengler, E.; Kao, W. J.; Heideman, W.; Peterson, R. E. Developmental Toxicity of Low Generation PAMAM Dendrimers in Zebrafish. *Toxicol. Appl. Pharmacol.* **2007**, *225*, 70–79.
10. Malik, N.; Evagorou, E. G.; Duncan, R. Dendrimer-Platinate: A Novel Approach to Cancer Chemotherapy. *Anticancer Drugs* **1999**, *10*, 67–76.
11. Malik, N.; Wiwattanapatapee, R.; Klopsch, R.; Lorenz, K.; Frey, H.; Weener, J. W.; Meijer, E. W.; Paulus, W.; Duncan, R. Dendrimers:: Relationship between Structure And Biocompatibility *In Vitro*, and Preliminary Studies on the Biodistribution of 125I-Labelled Polyamidoamine Dendrimers *in Vivo*. *J. Controlled Release* **2000**, *65*, 133–148.
12. Roberts, J. C.; Bhalgat, M. K.; Zera, R. T. Preliminary Biological Evaluation of Polyamidoamine (PAMAM) Starburst Dendrimers. *J. Biomed. Mater. Res.* **1996**, *30*, 53–65.
13. Jones, C. F.; Campbell, R. A.; Franks, Z.; Gibson, C. C.; Thiagarajan, G.; Vieira-de-Abreu, A.; Sukavaneshvar, S.; Mohammad, S. F.; Li, D. Y.; Ghandehari, H.; *et al*. Cationic PAMAM Dendrimers Disrupt Key Platelet Functions. *Mol. Pharm.* **2012**, *9*, 1599–1611.

14. Greish, K.; Thiagarajan, G.; Herd, H.; Price, R.; Bauer, H.; Hubbard, D.; Burckle, A.; Sadekar, S.; Yu, T.; Anwar, A. *et al*. Size and Surface Charge Significantly Influence the Toxicity of Silica and Dendritic Nanoparticles. *Nanotoxicology* **2012**, *6*, 713−723.
15. Siebenlist, K. R.; Mosesson, M. W. Progressive Cross-Linking of Fibrin Gamma Chains Increases Resistance to Fibrinolysis. *J. Biol. Chem.* **1994**, *269*, 28414–28419.
16. Jagadeeswaran, P. Zebrafish: A Tool to Study Hemostasis and Thrombosis. *Curr. Opin. Hematol.* **2005**, *12*, 149–152.
17. Khandekar, G.; Kim, S.; Jagadeeswaran, P. Zebrafish Thrombocytes: Functions and Origins. *Adv. Hematol.* **2012**, *2012*, 857058.
18. Lin, H. F.; Traver, D.; Zhu, H.; Dooley, K.; Paw, B. H.; Zon, L. I.; Handin, R. I. Analysis of Thrombocyte Development in CD41-GFP Transgenic Zebrafish. *Blood* **2005**, *106*, 3803–3810.
19. Hanumanthaiah, R.; Thankavel, B.; Day, K.; Gregory, M.; Jagadeeswaran, P. Developmental Expression of Vitamin K-Dependent Gamma-Carboxylase Activity in Zebrafish Embryos: Effect of Warfarin. In *Blood Cells, Mol. Dis.* **2001**, *27*, 992−999.
20. Jagadeeswaran, P.; Sheehan, J. P. Analysis of Blood Coagulation in the Zebrafish. *Blood Cells, Mol. Dis.* **1999**, *25*, 239−249.
21. Carradice, D.; Lieschke, G. J. Zebrafish in Hematology: Sushi or Science? *Blood* **2008**, *111*, 3331–3342.
22. Jagadeeswaran, P.; Sheehan, J. P.; Craig, F. E.; Troyer, D. Identification and Characterization of Zebrafish Thrombocytes. *Br. J. Hamaetol.* **1999**, *107*, 731−738.
23. Jagadeeswaran, P.; Gregory, M.; Johnson, S.; Thankavel, B. Haemostatic Screening and Identification of Zebrafish Mutants with Coagulation Pathway Defects: An Approach to Identifying Novel Haemostatic Genes in Man. *Br. J. Hamaetol.* **2000**, *110*, 946–956.
24. Jagadeeswaran, P.; Gregory, M.; Zhou, Y.; Zon, L.; Padmanabhan, K.; Hanumanthaiah, R., Characterization of Zebrafish Full-Length Prothrombin cDNA and Linkage Group Mapping. *Blood Cells, Mol. Dis.* **2000**, *26*, 479−489.
25. Sadekar, S.; Ghandehari, H. Transepithelial Transport and Toxicity of PAMAM Dendrimers: Implications for Oral Drug Delivery. *Adv. Drug Delivery Rev.* **2012**, *64*, 571–588.
26. Domanski, D. M.; Klajnert, B.; Bryszewska, M. Influence of PAMAM Dendrimers on Human Red Blood Cells. *Bioelectrochemistry* **2004**, *63*, 189–191.
27. Ottaviani, M. F.; Daddi, R.; Brustolon, M.; Turro, N. J.; Tomalia, D. A. Structural Modifications of DMPC Vesicles upon Interaction with Poly(amidoamine) Dendrimers Studied by CW-Electron Paramagnetic Resonance and Electron Spin−Echo Techniques. *Langmuir* **1999**, *15*, 1973–1980.
28. Jokiel, M.; Klajnert, B.; Bryszewska, M. Use of a Spectrofluorimetric Method to Monitor Changes of Human Serum Albumin Thermal Stability in the Presence of Polyamidoamine Dendrimers. *J. Fluoresc.* **2006**, *16*, 149–152.
29. Klajnert, B.; Cladera, J.; Bryszewska, M. Molecular Interactions of Dendrimers with Amyloid Peptides: pH Dependence. *Biomacromolecules* **2006**, *7*, 2186–2191.
30. Klajnert, B.; Pikala, S.; Bryszewska, M. Haemolytic Activity of Polyamidoamine Dendrimers and the Protective Role of Human Serum Albumin. *Proc. R. Soc. A* **2010**, *466*, 1527–1534.
31. Peters, T., Jr. Serum Albumin. *Adv. Protein Chem.* **1985**, *37*, 161–245.
32. Figge, J.; Rossing, T. H.; Fencl, V. The Role of Serum Proteins in Acid-Base Equilibria. *J. Lab. Clin. Med.* **1991**, *117*, 453–467.
33. Horbett, T. A. Chapter 13 Principles Underlying the Role of Adsorbed Plasma Proteins in Blood Interactions with Foreign Materials. *Cardiovasc. Pathol.* **1993**, *2*, 137–148.
34. Mertens, K. The Future of Plasma Derivatives. In *Transfus. Clin. Biol.* **2001**, *8*, 303−305.
35. Adkins, J. N.; Varnum, S. M.; Auberry, K. J.; Moore, R. J.; Angell, N. H.; Smith, R. D.; Springer, D. L.; Pounds, J. G. Toward a Human Blood Serum Proteome: Analysis by Multidimensional Separation Coupled with Mass Spectrometry. *Mol. Cell Proteomics* **2002**, *1*, 947–955.
36. Muthusamy, B.; Hanumanthu, G.; Suresh, S.; Rekha, B.; Srinivas, D.; Karthick, L.; Vrushabendra, B. M.; Sharma, S.; Mishra, G.; Chatterjee, P.; *et al*. Plasma Proteome Database as a Resource for Proteomics Research. *Proteomics* **2005**, *5*, 3531–3536.
37. Anderson, N. L.; Anderson, N. G.; Two-Dimensional Gel, A Database of Human Plasma Proteins. *Electrophoresis* **1991**, *12*, 883–906.
38. Wiles, T. J.; Bower, J. M.; Redd, M. J.; Mulvey, M. A. Use of Zebrafish to Probe the Divergent Virulence Potentials and Toxin Requirements of Extraintestinal Pathogenic Escherichia Coli. *PLoS Pathog.* **2009**, *5*, e1000697.
39. Traver, D.; Paw, B. H.; Poss, K. D.; Penberthy, W. T.; Lin, S.; Zon, L. I. Transplantation and *in Vivo* Imaging of Multilineage Engraftment in Zebrafish Bloodless Mutants. *Nat. Immunol.* **2003**, *4*, 1238−1246.
40. Campbell, R. A.; Overmyer, K. A.; Selzman, C. H.; Sheridan, B. C.; Wolberg, A. S. Contributions of Extravascular and Intravascular Cells to Fibrin Network Formation, Structure, and Stability. *Blood* **2009**, *114*, 4886–4896.
41. Campbell, R. A.; Overmyer, K. A.; Bagnell, C. R.; Wolberg, A. S. Cellular Procoagulant Activity Dictates Clot Structure and Stability as a Function of Distance from the Cell Surface. *Arterioscler. Thromb. Vasc. Biol.* **2008**, *28*, 2247–2254.
42. Assemi, S.; Tadjiki, S.; Donose, B. C.; Nguyen, A. V.; Miller, J. D. Aggregation of Fullerol $C_{60}(OH)_{24}$ Nanoparticles as Revealed Using Flow Field-Flow Fractionation and Atomic Force Microscopy. *Langmuir* **2010**, *26*, 16063–16070.